Theoretical and Kinetic Study of the Reactions of Ketones with $H\dot{O}_2$ Radicals. Part I: Abstraction Reaction Channels

Jorge Mendes,* Chong-Wen Zhou,* and Henry J. Curran

Combustion Chemistry Centre, National University of Ireland, Galway, Ireland.

E-mail: j.mendesferreira1@nuigalway.ie; chongwen.zhou@nuigalway.ie

*To whom correspondence should be addressed

Abstract

This work presents an *ab-initio* and chemical kinetic study of the reaction mechanisms of hydrogen atom abstraction by the $H\dot{O}_2$ radical on five ketones: dimethyl, ethyl methyl, *n*-propyl methyl, *iso*-propyl methyl and *iso*-butyl methyl ketones. The Møller–Plesset method using the 6-311G(d,p) basis set has been used in the geometry optimization and the frequency calculation for all the species involved in the reactions, as well as the hindrance potential description for reactants and transition states. Intrinsic reaction co-ordinate calculations were carried out to validate all the connections between transition states and local minima. Energies are reported at the CCSD(T)/cc-pVTZ//MP2/6-311G(d,p) level of theory. The CCSD(T)/cc-pV*X*Z method (*X* = D, T, Q) was used for the reaction mechanism of dimethyl ketone + $H\dot{O}_2$ radical in order to benchmark the computationally less expensive method of CCSD(T)/cc-pVTZ//MP2/6-311G(d,p). High-pressure limit rate constants have been calculated for all the reaction channels by conventional transition state theory with asymmetric Eckart tunneling corrections and 1-D hindered rotor approximations in the temperature range 500–2000 K.

Keywords

ab-initio, ketones, hydroperoxyl radical, abstraction, oxygenated fuels

Introduction

Ketones are one of the most common pollutants as they are used in industry as paints, solvents, *etc*. In both the atmosphere and in combustion systems ketones play an important role. They can be formed as intermediate products in hydrocarbon oxidation processes during combustion.[1] Due to their fluorescent properties they are also used as fuel tracers in order to measure, in a non-invasive way, the temperature fields and reactant composition of intractable environments such as internal combustion engines.[1] Understanding this reactivity, particularly at temperatures above 500 K, is important in order to develop successful detailed chemical kinetic models suitable for application to combustion systems.[1] There is an interest in studying the influence of the carbonyl group in ketones (dimethyl, ethyl methyl, *n*-propyl methyl, *iso*-propyl methyl and *iso*-butyl methyl ketones) on the reactivity of the different types of hydrogen atoms, primary (1°), secondary (2°), or tertiary (3°), on the fuel molecule undergoing abstraction by the $H\dot{O}_2$ radical, because this radical is in high concentration at intermediate temperatures (800–1300 K) and high pressures ($>$ 10 atm) in combustion systems.

In the combustion temperature regime, hydrogen atom abstraction reactions by small radicals such as $\dot{O}$, $\dot{H}$, $\dot{O}H$, $H\dot{O}_2$ and $\dot{C}H_3$ from fuel molecules are always important in the oxidation of fuels. Hydrogen atom abstraction by an $H\dot{O}_2$ radical will result in the formation of hydrogen peroxide (H_2O_2) and a ketone radical. H_2O_2 subsequently decomposes to form two $\dot{O}H$ radicals which are highly reactive:

$$RH + H\dot{O}_2 \rightarrow \dot{R} + H_2O_2$$

$$H_2O_2\ (+M) \rightarrow \dot{O}H + \dot{O}H\ (+M)$$

The reaction of an $H\dot{O}_2$ radical with a ketone proceeds through a stepwise mechanism involving reactant complexes (RC) formed in the entrance channel and product complexes (PC) formed in the exit channel. In our previous work[1] we have determined that two conformers exist for the reactions of EMK with an $\dot{O}H$ radical (*gauche* and *trans*) which have similar chemical properties. We have also determined that iPMK has two conformers when reacting with an $\dot{O}H$ radical which have quite

similar kinetic behavior.[1] Therefore, only the lowest energy reactant conformers are used in every reaction process studied in this work. We have carried out rate constant calculations for hydrogen atom abstraction at the different sites of dimethyl (DMK), ethyl methyl (EMK), *n*-propyl methyl (nPMK), *iso*-propyl methyl (iPMK) and *iso*-butyl methyl (iBMK) ketones, Fig. 1.

Several authors have performed studies of the reactions of ketones with $H\dot{O}_2$ radicals. Theoretical studies have been performed by Cours *et al.*,[2] Hermans *et al.*,[3,4] and Aloisio *et al.*[5] Moreover, Grieman *et al.*,[6] Gierczak *et al.*,[7] and Dillon *et al.*[8] have experimentally measured the rate of reaction for the addition reactions of an $H\dot{O}_2$ radical to ketones.

Cours *et al.* have studied theoretically both the abstraction and addition pathways of the reactions of DMK with the $H\dot{O}_2$ radical but rate constants were only calculated for adduct formation and decomposition at 200–298 K, and were not reported for hydrogen atom abstraction. Hermans *et al.* have calculated the forward and reverse coefficients of several reactions, including the adduct formation for the addition of an $H\dot{O}_2$ radical to DMK in the temperature range 200–600 K. Aloisio *et al.* have performed theoretical studies of the formation of a hydrogen-bonded complex in the reactions of several molecules with the $H\dot{O}_2$ radical, including DMK. Grieman *et al.* have determined experimentally the equilibrium constants of the addition reactions of the $H\dot{O}_2$ radical to DMK in the temperature range 215–272 K. Gierczak *et al.* have performed experimental studies of the addition reactions of $H\dot{O}_2$ radicals to several ketones, including DMK at 298 and 372 K and EMK and nPMK at 297 and 372 K. Dillon *et al.* have carried out experimental and theoretical studies of the addition reactions of an $H\dot{O}_2$ radical to DMK at several temperatures between 207 and 298 K.

In this work, we describe a systematic study of the reaction mechanisms, potential energy surfaces and high-pressure limit rate constant calculations of hydrogen atom abstraction reactions of ketones with $H\dot{O}_2$ radicals.

Apart from the hydrogen atom abstraction reaction channels, we find that the $H\dot{O}_2$ addition channel with lower barrier height will also be favored. In the addition channels, the 'OO' of the $H\dot{O}_2$ radical adds to the carbonyl carbon of the ketone and the 'H' adds to the carbonyl oxygen, to

form an intermediate adduct.[9]

Computational methods

The Møller–Plesset[10] (MP2) method using the 6-311G(d,p) basis set has been employed in the geometry optimizations, frequency calculations and hindered-rotor scans of reactants and transition states. MP2 is a good compromise between accuracy and computational cost.[11] Intrinsic Reaction Co-ordinate[12] (IRC) calculations were performed in order to confirm the connection between transition state and local minima. Local minima, or first-order saddle points, were determined by performing vibrational frequency analyses. The coupled-cluster approach with single and double substitutions, including perturbative estimates of the connected triples or CCSD(T) method,[13] was used in order to obtain more reliable energies along the potential energy surface (PES) for the hydrogen atom abstraction reactions of DMK + $H\dot{O}_2$ radical. The CCSD(T) method was used with the cc-pV*X*Z basis set and was extrapolated to the complete basis set (CBS) limit using the three-parameter equation provided by Peterson *et al.*:[14]

$$E(X) = E_{CBS} + A \exp[-(X-1)] + B \exp[-(X-1)^2]$$

where X = 2, 3, 4 for the D, T, Q extrapolation.

T1 diagnostics was investigated in the CCSD(T) energy calculations for all of the species involved in the reaction mechanisms of the ketones with the $H\dot{O}_2$ radical, and are all almost equivalent to, or less than, the 0.02 critical value. This indicates that the single reference method provides an adequate description of the wavefunction.[15] CCSD(T)/cc-pV*X*Z single point energy calculations for all of the species involved in the reactions of DMK + $H\dot{O}_2$ radical are based on the geometries obtained at MP2/6-311G(d,p) and B3LYP/6-311G(2d,d,p) levels of theory. Energies obtained by the CBS-QB3[16] method were benchmarked against CCSD(T)/CBS//B3LYP/6-311G(2d,d,p) energies. CBS-QB3 underestimates the energies of the transition states by 2–3 kcal mol^{-1}. The CCSD(T)/cc-pVTZ//MP2/6-311G(d,p) energies were benchmarked against the energies obtained by the CCSD(T)/CBS//MP2/6-311G(d,p) level of theory and are within 0.4 kcal mol^{-1} for the transition states. Therefore, these energies are used in the rate constant calculations as they are

in substantially better agreement with the corresponding high-level energy calculations in contrast to the CBS-QB3 ones. Unless otherwise stated, all energies are reported as zero-point corrected electronic energies. All of the harmonic frequencies were scaled by 0.9496 as recommended by Merrick *et al.*[17] which are the basis for all single point energy (SPE) calculations and rate constant calculations. All quantum chemistry calculations were performed using Gaussian-09[18] with visualization and determination of geometrical parameters using ChemCraft.[19]

Potential Energy Surface

To clarify the labels we use and the different types of hydrogen atoms in this work we give Fig. 1 and Table 1. Optimized geometries of the ketones in this study are shown in Fig. 2. Table S1 in the Supporting Information details the CCSD(T)/cc-pV*X*Z//MP2/6-311G(d,p) (*X* = D, T, Q) single point energy calculations and extrapolation to the complete basis set limit, CCSD(T)/CBS//MP2/6-311G(d,p), for the reactions of DMK with an $H\dot{O}_2$ radical. Table S2 in the Supporting Information details the geometry co-ordinates and frequencies of all of the species in the reactions.

Several reactant complexes with the same energy, quite similar geometries and frequencies have been located in the reaction systems of EMK, nPMK, iPMK and iBMK when they react with an $H\dot{O}_2$ radical. For simplicity, only one of them is shown in the potential energy diagrams.

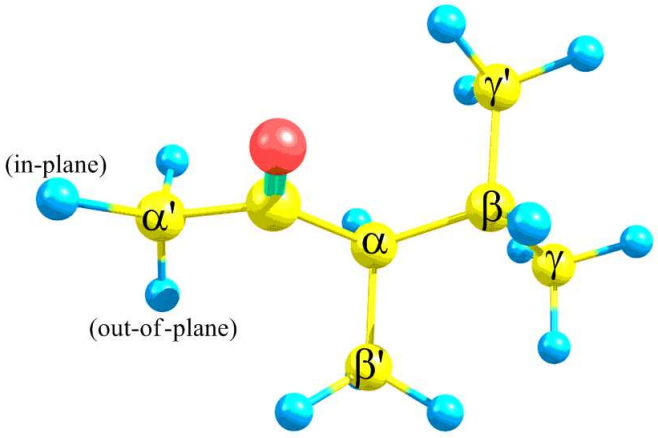

Figure 1: Labels used in this work.

Table 1: Types of hydrogen atoms present in this work.

	α'	α	β	γ
DMK	1°	1°	–	–
EMK	1°	2°	1°	–
nPMK	1°	2°	2°	1°
iPMK	1°	3°	1°	–
iBMK	1°	2°	3°	1°

Multiple independent transition states have been found. When the $H\dot{O}_2$ radical abstracts an in-plane hydrogen atom, an in-plane transition state is formed where a hydrogen bond exists between the hydrogen of the hydroperoxyl radical and the oxygen of the carbonyl group of the ketone. When an out-of-plane hydrogen atom is abstracted, an out-of-plane transition state is formed where there is no hydrogen bond present. Due to the formation of this hydrogen bond, the in-plane transition state will have a lower entropy than the out-of-plane transition state, which will affect the rate constants at high temperatures. We consider the contribution of both types of transition states in our calculations. Fig. 3 shows α' out-of-plane (TS1a) and in-plane (TS2a) transition states for DMK, α out-of-plane (TS3b) and in-plane (TS4b) transition states for EMK, β out-of-plane (TS5d) and in-plane (TS6d) transition states for iPMK and γ out-of-plane (TS7c) and in-plane (TS8e) transition states for nPMK and iBMK, respectively.

At the α' position all hydrogen atoms are 1° for all of the species in this study, while hydrogen atoms at the α position are 1° for DMK, 2° for EMK, nPMK and iBMK and 3° in the case of iPMK; at the β position, the hydrogen atoms are 1° for EMK and iPMK, 2° for nPMK and 3° for iBMK; γ hydrogen atoms are 1° for both nPMK and iBMK (see Table 1). The potential energy surfaces (energies in kcal mol^{-1}) obtained at CCSD(T)/cc-pVTZ//MP2/6-311G(d,p), CCSD(T)/CBS//MP2/6-311G(d,p), CBS-QB3 and CCSD(T)/CBS//B3LYP/6-311G(2d,d,p) levels of theory are shown in Fig. 4 for DMK and at the CCSD(T)/cc-pVTZ//MP2/6-311G(d,p) level of theory in Fig. 5 for EMK, in Fig. 6 for nPMK, in Fig. 7 for iPMK and in Fig. 8 for iBMK.

For most of the pre and post-reaction complexes involved in the reaction mechanisms of ketones with the $H\dot{O}_2$ radical, a hydrogen bond is formed between the hydrogen atom of the hydroperoxyl radical and the oxygen atom of the ketone. The complexes that do not form a hydrogen

bond undergo a weaker *van der waals* interaction when they are formed in the entrance and exit channels. The O–H bond distances are in the range of 1.7–1.8 Å for the reactant complexes, 1.8–2.0 Å for the product complexes and 2.0–2.3 Å for the in-plane transition states. Most of these hydrogen bonds are strong with a few weaker ones, possibly due to the hydrogen atom not bearing sufficient positive charge to interact strongly with the oxygen atom. The radical products formed upon abstraction by the $H\dot{O}_2$ radical have higher energies than the corresponding product complexes and, when comparing their geometries, they do not differ greatly (Table S2 in the Supporting Information).

Abstraction of a hydrogen atom at the α' position

Primary hydrogen atom abstraction by the $H\dot{O}_2$ radical at the α' position in ketones occurs similarly for DMK, EMK, nPMK, iPMK and iBMK. Two categories of hydrogen atoms are present; one in-plane and the other out-of-plane and will form in- and out-of-plane transition states when reacting with the $H\dot{O}_2$ radical, respectively.

Potential energy diagrams of these reaction processes are shown in Figs. 4 – 8. Reactant complexes for the reactions of ketones with the $H\dot{O}_2$ radical have all been identified in the entrance channels for the abstraction of an α' 1° hydrogen atom and are in the range of -9.8 to -9.1 kcal mol^{-1}. The reactant complexes RC1a, RC1b, RC1c, RC1d and RC1e will go through TS1a for DMK, TS1b for EMK, TS1c for nPMK, TS1d for iPMK and TS1e for iBMK which are labeled as out-of-plane transition states. RC1a, RC2b, RC2c, RC2d and RC2e proceed through TS2a for DMK, TS2b for EMK, TS2c for nPMK, TS2d for iPMK and TS2e for iBMK which are labeled as in-plane transition states. TS1a and TS2a have energy barriers of 29.7 and 29.9 kcal mol^{-1}, respectively. TS1b and TS2b have energy barriers of 29.3 and 29.5 kcal mol^{-1}, respectively; TS1c and TS2c have barriers of 29.0 and 29.6 kcal mol^{-1}, respectively. TS1d and TS2d have barriers of 28.2 and 29.2 kcal mol^{-1}, respectively. TS1e and TS2e have barriers of 29.3 and 29.6 kcal mol^{-1}, respectively. Product complexes are formed in the exit channel of all of the ketones when the $H\dot{O}_2$ radical abstracts an α' 1° hydrogen atom. For both transition states in the reaction mechanism of DMK, the product complex PC1a is formed in the exit channel with a relative energy of 3.5 kcal

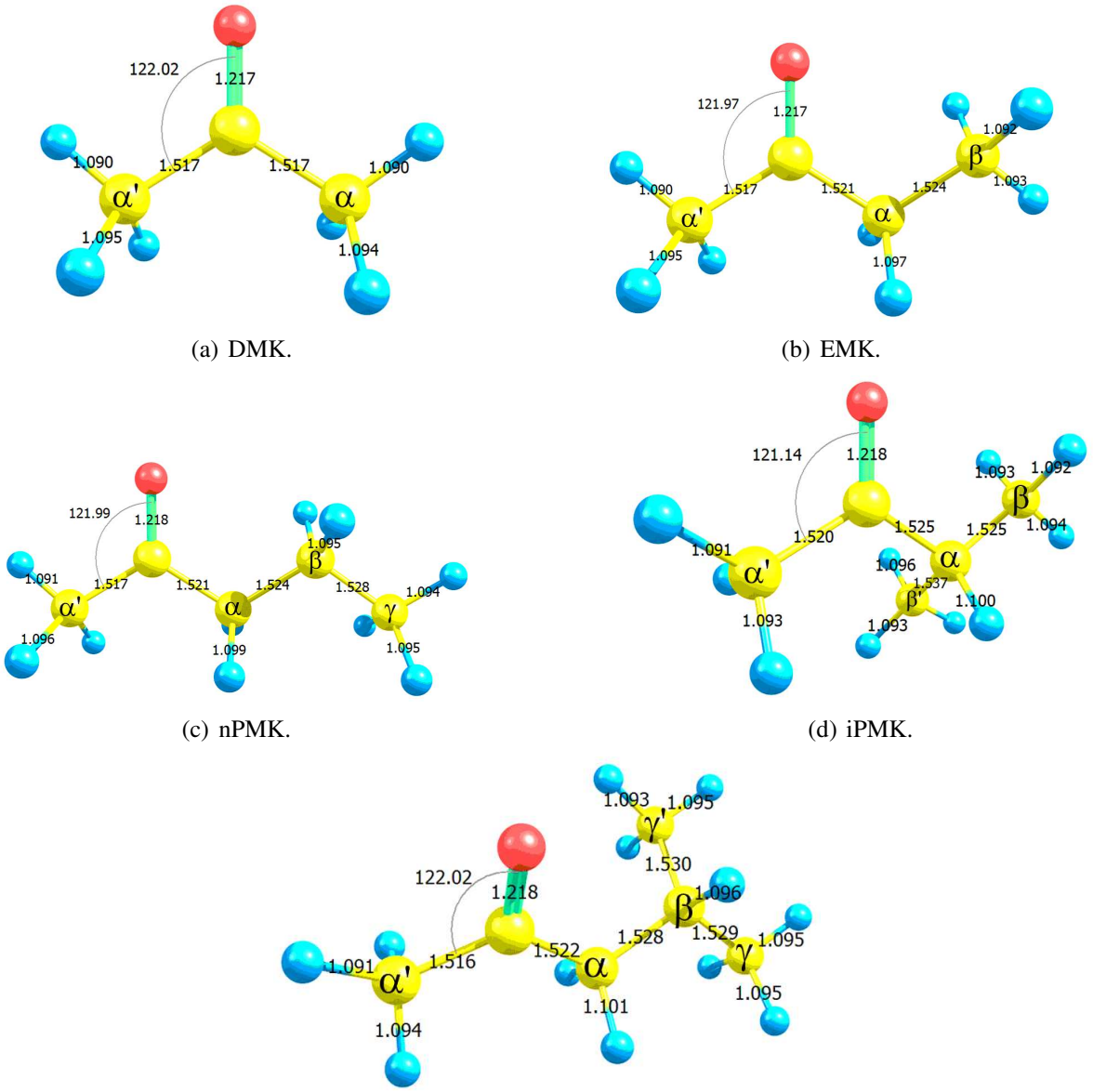

(a) DMK.

(b) EMK.

(c) nPMK.

(d) iPMK.

(e) iBMK.

Figure 2: Optimized geometries of DMK, EMK, nPMK, iPMK and iBMK at MP2/6-311G(d,p) showing the different types of hydrogen atoms: DMK primary α' and α H-atoms; EMK primary α' and β H-atoms and secondary α H-atoms; nPMK primary α' and γ H-atoms, secondary α and β H-atoms; iPMK primary α', β and β' H-atoms and tertiary α H-atom; iBMK primary α', γ and γ' H-atoms, secondary α H-atoms and tertiary β H-atoms.

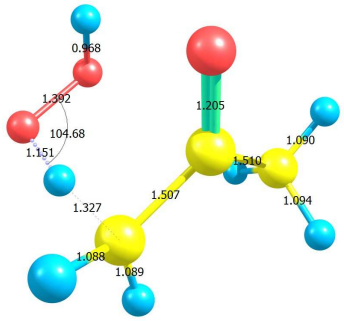

(a) DMK TS1a (out-of-plane).

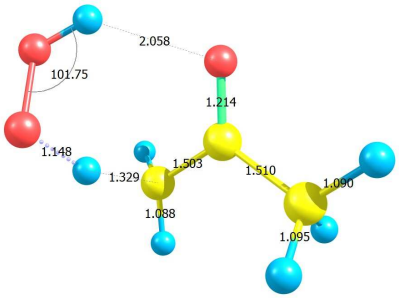

(b) DMK TS2a (in-plane).

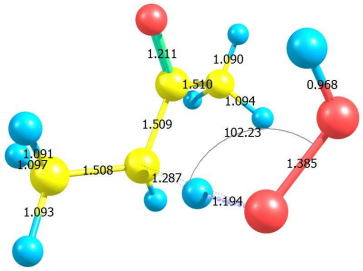

(c) EMK TS3b (out-of-plane).

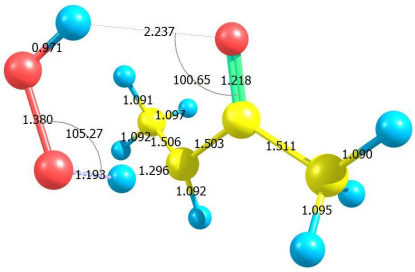

(d) EMK TS4b (in-plane).

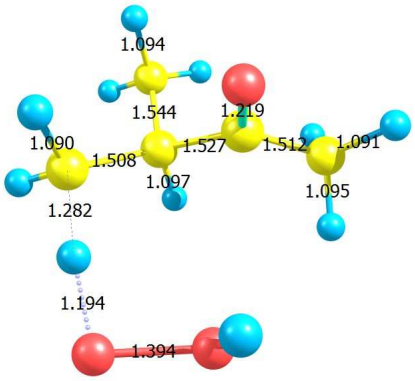

(e) iPMK TS5d (out-of-plane).

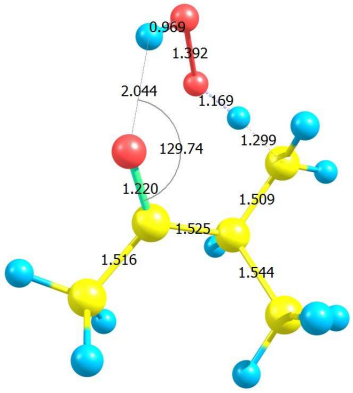

(f) iPMK TS6d (in-plane).

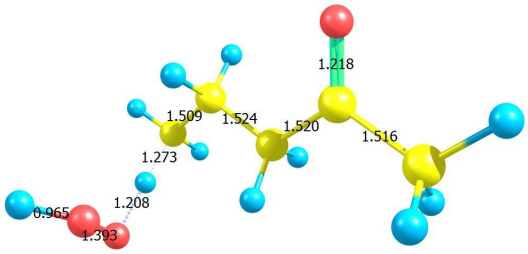

(g) nPMK TS7c (out-of-plane).

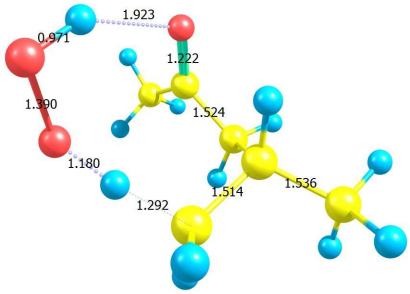

(h) iBMK TS8e (in-plane).

Figure 3: Optimized geometries of transition states (α' for DMK, α for EMK, β for iPMK and γ for nPMK and iBMK) for the hydrogen atom abstraction reactions of ketones with the $H\dot{O}_2$ radical at MP2/6-311G(d,p).

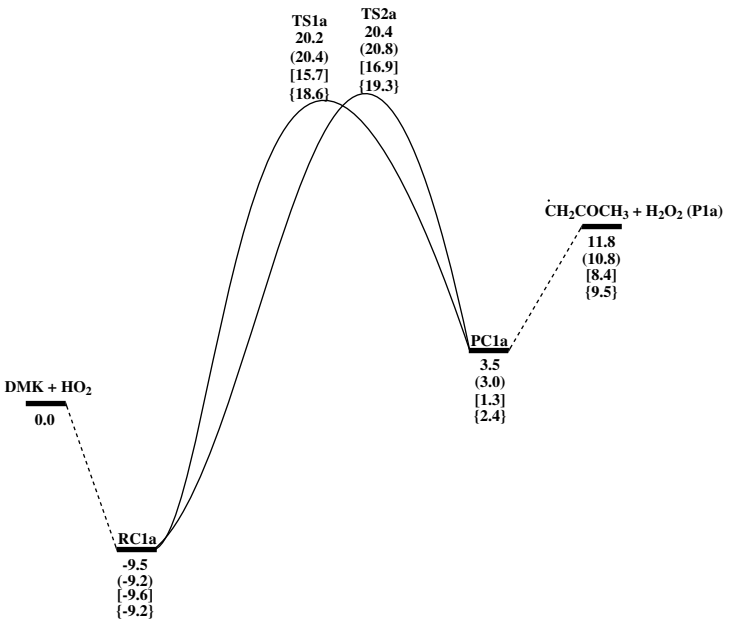

Figure 4: Potential energy surface of the reactions of DMK + $H\dot{O}_2$ radical at CCSD(T)/cc-pVTZ//MP2/6-311G(d,p), CCSD(T)/CBS//MP2/6-311G(d,p) (in round brackets), CBS-QB3 (in square brackets) and CCSD(T)/CBS//B3LYP/6-311G(2d,d,p) (in curly brackets), in kcal mol^{-1}.

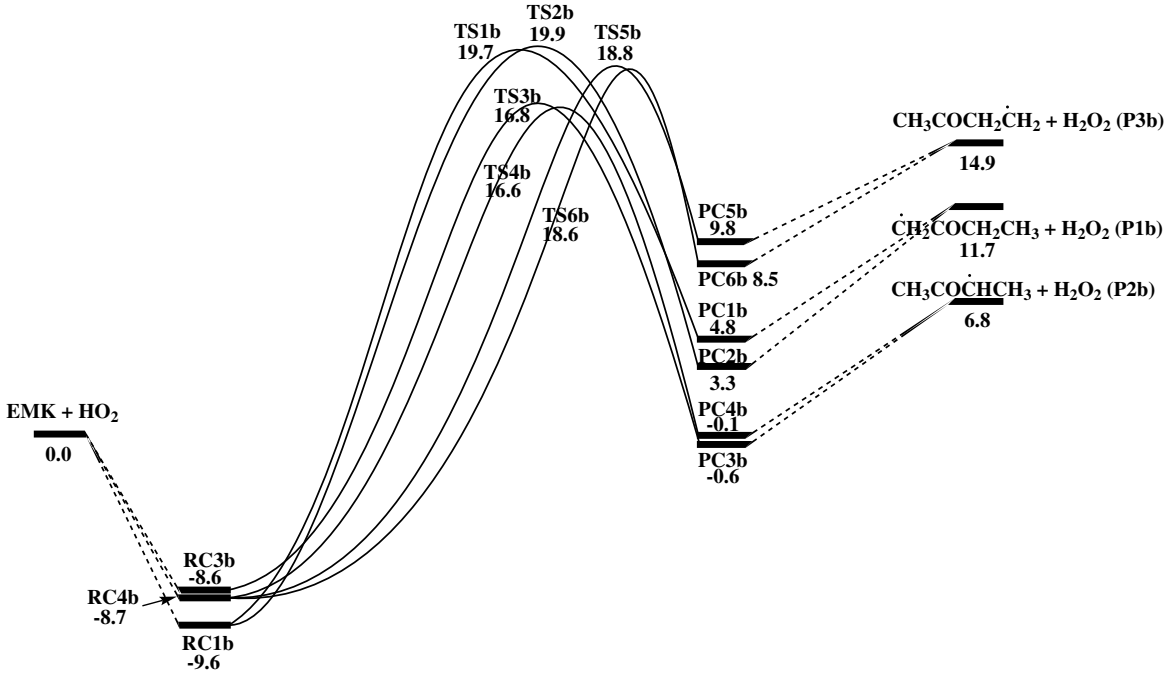

Figure 5: Potential energy surface of the reactions of EMK + $H\dot{O}_2$ radical at CCSD(T)/cc-pVTZ//MP2/6-311G(d,p) level of theory in kcal mol^{-1}.

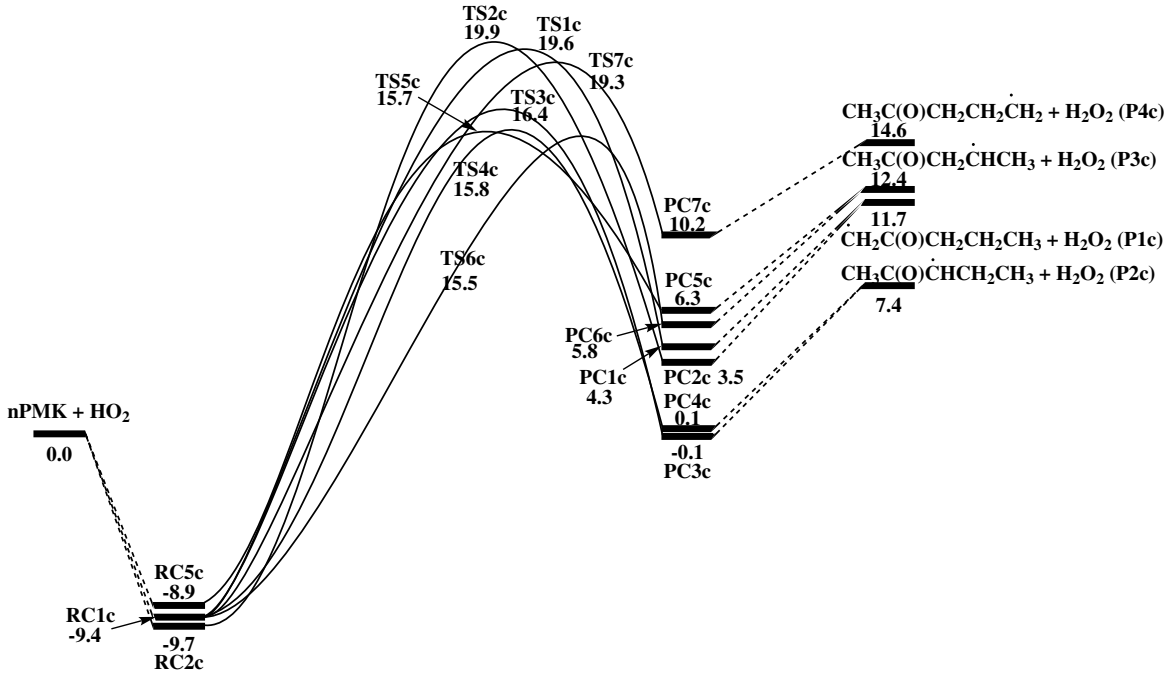

Figure 6: Potential energy surface of the reactions of nPMK + $H\dot{O}_2$ radical at CCSD(T)/cc-pVTZ//MP2/6-311G(d,p) level of theory in kcal mol^{-1}.

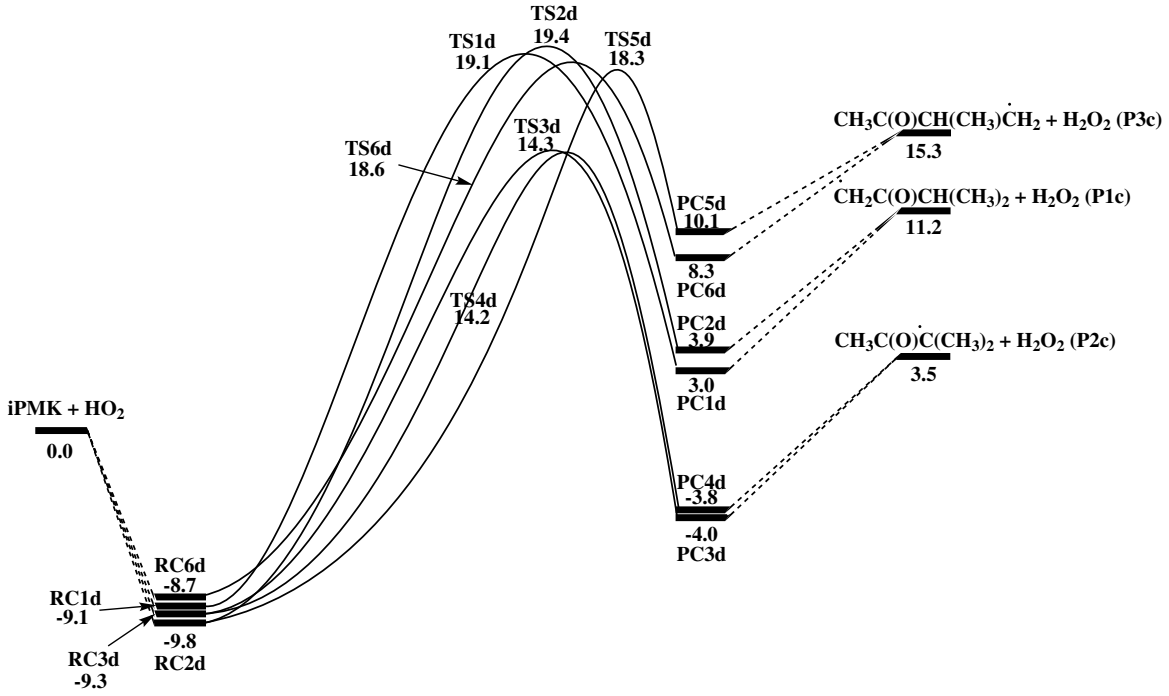

Figure 7: Potential energy surface of the reactions of iPMK + $H\dot{O}_2$ radical at CCSD(T)/cc-pVTZ//MP2/6-311G(d,p) level of theory in kcal mol^{-1}.

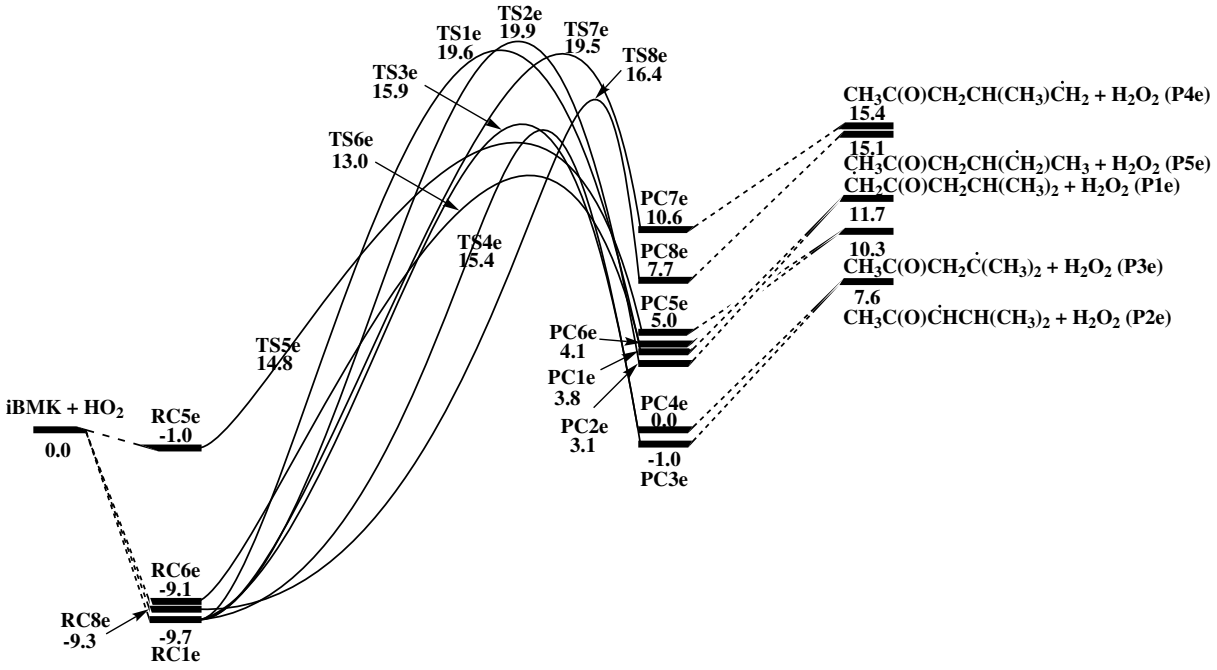

Figure 8: Potential energy surface of the reactions of iBMK + $H\dot{O}_2$ radical at CCSD(T)/cc-pVTZ//MP2/6-311G(d,p) level of theory in kcal mol^{-1}.

mol^{-1}. For the out-of-plane transition states in the reactions of EMK, nPMK, iPMK and iBMK with the $H\dot{O}_2$ radical, PC1b at 4.8 kcal mol^{-1}, PC1c at 4.3 kcal mol^{-1}, PC1d at 3.0 kcal mol^{-1} and PC1e at 3.8 kcal mol^{-1} will be formed, respectively. Product complexes PC2b at 3.3 kcal mol^{-1}, PC2c at 3.5 kcal mol^{-1}, PC2d at 3.9 kcal mol^{-1} and PC2e at 3.1 kcal mol^{-1} were identified in the exit channels of the in-plane transition states TS2b, TS2c, TS2d and TS2e, respectively. Abstraction of a hydrogen atom from the α' position leads to the formation of H_2O_2 and a 1° α' radical for all of the ketones: P1a for DMK at 11.8 kcal mol^{-1}, P1b for EMK at 11.7 kcal mol^{-1}, P1c for nPMK at 11.7 kcal mol^{-1}, P1d for iPMK at 11.2 kcal mol^{-1} and P1e for iBMK at 11.7 kcal mol^{-1}.

Abstraction of a hydrogen atom at the α position

For the α position in the ketones (ethyl, *n*-propyl, *iso*-propyl or *iso*-butyl groups), a secondary hydrogen atom in EMK, nPMK and iBMK and a tertiary hydrogen atom for iPMK will be abstracted when reacting with the $H\dot{O}_2$ radical (Fig. 1, Table 1).

As for the hydrogen atom abstraction at the α' position, a reactant complex is formed in the entrance channel for both the in-plane and the out-of-plane transition states. For the α hydrogen atom abstraction, reactant complexes RC3b and RC4b, at -8.6 and -8.7 kcal mol^{-1}, respectively, for EMK, RC3c and RC4c, both at -9.4 kcal mol^{-1} for nPMK, RC3d and RC4d, both at -9.3 kcal mol^{-1} for iPMK and RC3e and RC4e, both at -9.7 kcal mol^{-1} for iBMK have all been identified in the entrance channels. RC3b, RC3c, RC3d and RC3e will all go through an out-of-plane transition state, with energy barriers of 25.4 kcal mol^{-1} for TS3b in EMK, 25.8 kcal mol^{-1} for TS3c in nPMK, 23.6 kcal mol^{-1} for TS3d in iPMK and 25.6 kcal mol^{-1} for TS3e in iBMK, respectively. RC4b, RC4c, RC4d and RC4e will all proceed through an in-plane transition state, with energy barriers of 25.3 kcal mol^{-1} for TS4b in EMK, 25.2 kcal mol^{-1} for TS4c in nPMK, 23.5 kcal mol^{-1} for TS4d in iPMK and 25.1 kcal mol^{-1} for TS4e in iBMK, respectively. TS3b, TS3c, TS3d and TS3e lie 16.8, 16.4, 14.3 and 15.9 kcal mol^{-1} above the reactants, respectively, while TS4b, TS4c, TS4d and TS4e lie 16.6, 15.8, 14.2 and 15.4 kcal mol^{-1} above the reactants, respectively.

Similar to the α' position, product complexes are formed in the exit channels (Figs. 4 – 8). Abstraction of a hydrogen atom from the α position leads to the formation of H_2O_2 and a 2° α radical for EMK (P2b at 6.8 kcal mol^{-1}), nPMK (P2c at 7.4 kcal mol^{-1}) and iBMK (P2e at 7.6 kcal mol^{-1}) and a 3° α radical for iPMK (P2d at 3.5 kcal mol^{-1}).

Abstraction of a hydrogen atom at the β, β' and γ, γ' positions

For β, β' and γ, γ' hydrogen atom abstraction, the same behavior is observed as with α' and α positions where a reactant complex is formed in the entrance channel and a product complex in the exit channel. Abstraction from the β position of EMK, β or β' positions of iPMK, β and γ or γ' positions of iBMK will also form in- and out-of-plane transition states. However, the same does not occur for the γ position of nPMK where an in-plane transition state is not formed due to the distance of the $H\dot{O}_2$ radical from the carbonyl group of the ketone, precluding the formation of a hydrogen bond. Therefore, only an out-of-plane transition state is formed, Fig. 3(g).

Abstraction at the β or β' positions will form H_2O_2 and a 1° β radical for EMK (P3b at 14.9

kcal mol^{-1}) and iPMK (P3d at 15.3 kcal mol^{-1}), a 2° β radical for nPMK (P3c at 12.4 kcal mol^{-1}) and a 3° β radical for iBMK (P3e at 10.3 kcal mol^{-1}).

Abstraction from the γ or γ' positions will generate H_2O_2 and a 1° γ radical for nPMK (P4c at 14.6 kcal mol^{-1}) and two similar 1° γ radicals for iBMK (P4e at 15.4 kcal mol^{-1}, from TS7e and P5e at 15.1 kcal mol^{-1}, from TS8e).

Rate constant calculations

The main objective of this study lies in the determination of the high-pressure limit rate constants of the hydrogen atom abstraction reactions by the $H\dot{O}_2$ radical on ketones based on the above potential energy surfaces and reaction mechanisms. Conventional transition state theory with asymmetric Eckart tunneling correction[20] as implemented in Variflex v2.02m[21] is employed to calculate the high-pressure limit rate constants in the combustion temperature range from 500–2000 K. The formation of the reactant complexes and product complexes will narrow the tunneling barrier which will accelerate the tunneling effect and furthermore the rate constants. Tunneling is important at lower temperatures (500–1000 K) in our work, especially for the light hydrogen atom transfer reaction processes. Fig.10(c) shows a comparison of the α' 1° hydrogen atom abstraction rate constants for the reactions of DMK with the $H\dot{O}_2$ radical with and without tunneling correction. When the tunneling correction is included, the rate constants increase by a factor of 4.7 at 500 K. The low-frequency torsional modes were treated as 1-D hindered rotors using the Pitzer-Gwinn-like[22] approximation. The torsional treatment is difficult at present because sometimes the coupling between the adjacent internal rotations or the ones between internal rotation and external rotation are too strong to be separated. The 1-D hindered rotor treatment is the best we can do at the moment as most of the internal rotations in this work are separable. Truhlar and co-workers[23,24] have developed the multi-structure method to deal with the torsional coupling problem, and their application to the hydrogen atom abstraction reaction of *n*-Butanol + $H\dot{O}_2$ shows that their multi-structure method results are quite close to our 1-D hindered rotor treatment results in both α and γ hydrogen atom abstraction rate constants.[25] The hindrance potentials were determined for every geometry

around every possible dihedral angle. The remaining modes were treated as harmonic oscillators. These rate constants have been fitted to a three parameter modified Arrhenius equation (Table 2) with an average error of approximately 4.5% and a maximum error of no more than 8.3%, and are reported on a per hydrogen atom basis in $cm^3\ mol^{-1}\ s^{-1}$.

Table 2: Rate constants on a per hydrogen atom basis in $cm^3\ mol^{-1}\ s^{-1}$ for the different abstraction positions of DMK, EMK, nPMK, iPMK and iBMK, from 500–2000 K.

DMK + $H\dot{O}_2$

$k(\text{DMK } \alpha') = 6.62\times10^{-4}\ T^{4.51}\ \exp(-8372/T)$ (1)

EMK + $H\dot{O}_2$

$k(\text{EMK } \alpha') = 1.86\times10^{-3}\ T^{4.32}\ \exp(-8248/T)$ (2)
$k(\text{EMK } \alpha) = 4.21\times10^{-2}\ T^{3.93}\ \exp(-6738/T)$ (3)
$k(\text{EMK } \beta) = 2.06\times10^{-5}\ T^{4.91}\ \exp(-7086/T)$ (4)

nPMK + $H\dot{O}_2$

$k(\text{nPMK } \alpha') = 1.38\times10^{-2}\ T^{4.07}\ \exp(-8179/T)$ (5)
$k(\text{nPMK } \alpha) = 1.78\times10^{-1}\ T^{3.69}\ \exp(-6592/T)$ (6)
$k(\text{nPMK } \beta) = 5.75\times10^{-4}\ T^{4.43}\ \exp(-5719/T)$ (7)
$k(\text{nPMK } \gamma) = 1.48\times10^{-1}\ T^{3.88}\ \exp(-7958/T)$ (8)

iPMK + $H\dot{O}_2$

$k(\text{iPMK } \alpha') = 4.39\times10^{-3}\ T^{4.22}\ \exp(-8096/T)$ (9)
$k(\text{iPMK } \alpha) = 8.48\times10^{-1}\ T^{3.53}\ \exp(-5725/T)$ (10)
$k(\text{iPMK } \beta, \beta') = 3.98\times10^{-4}\ T^{4.56}\ \exp(-7642/T)$ (11)

iBMK + $H\dot{O}_2$

$k(\text{iBMK } \alpha') = 7.87\times10^{-2}\ T^{3.83}\ \exp(-8171/T)$ (12)
$k(\text{iBMK } \alpha) = 4.70\times10^{-3}\ T^{4.13}\ \exp(-6131/T)$ (13)
$k(\text{iBMK } \beta) = 5.69\times10^{+1}\ T^{2.99}\ \exp(-5550/T)$ (14)
$k(\text{iBMK } \gamma, \gamma') = 1.93\times10^{-1}\ T^{3.75}\ \exp(-7953/T)$ (15)

The hydrogen bond formed in the in-plane transition state ties up rotors, thus decreasing the entropy and the frequency factor for reaction, resulting in lower rate constants at high temperatures relative to reactions where no hydrogen bonding occurs. At lower temperatures, the higher energy barriers (Table 5) for the hydrogen atom abstraction reactions results in slower rate constants, when compared to the reactions of alkanes + $H\dot{O}_2$ radical calculated by Aguilera-Iparraguirre *et al.*[26] The temperature dependence of the calculated rate constants is shown in Figs. 9 and 10(a) for the

Table 3: Recommended fit parameters, A, n and E, according to hydrogen atom type and position relative to the carbonyl group of the ketone, on a per-hydrogen atom basis in $cm^3\ mol^{-1}\ s^{-1}$, from 500–2000 K.

Hydrogen atom type	A	n	E
Primary, α'	3.52×10^{-3}	4.25	-8120
Secondary, α	2.54×10^{-2}	3.95	-6458
Tertiary, α	8.48×10^{-1}	3.53	-5725
Primary, β	7.29×10^{-5}	4.76	-7330
Secondary, β	5.75×10^{-4}	4.43	-5719
Tertiary, β	$5.69 \times 10^{+1}$	2.99	-5550
Primary, γ	1.48×10^{-1}	3.84	-7952

Table 4: Total rate constants fit parameters, A, n and E, in $cm^3\ mol^{-1}\ s^{-1}$.

	A	n	E
DMK	3.97×10^{-3}	4.51	-8372
EMK	2.16×10^{-4}	4.83	-6461
nPMK	3.67×10^{-4}	4.80	-6019
iPMK	1.06×10^{-7}	5.75	-4664
iBMK	2.68×10^{-5}	5.04	-4587

α' (1°), α (2°), α (3°), β (1°), β (2°), β (3°) and γ (1°) hydrogen atom abstraction reactions of ketones with the $H\dot{O}_2$ radical. Included is a comparison with the rate constants derived by Aguilera-Iparraguirre *et al.*[26] and Carstensen *et al.*,[27] for the hydrogen atom abstraction reactions of alkanes with $H\dot{O}_2$ radicals.

Fig. 9(a) shows a plot of the calculated rate constants for abstraction of an α' 1° hydrogen atom from DMK, EMK, nPMK, iPMK and iBMK and a comparison with those calculated by Aguilera-Iparraguirre *et al.* and Carstensen *et al.*, from alkanes. A trend is observed for all of the ketones investigated where the reactions are slower by approximately an order of magnitude throughout the complete temperature range when compared to those with alkanes calculated by Aguilera-Iparraguirre *et al.* At lower temperatures (500 K) this is due to the higher energy barriers (Table 5) of the reactions of ketones + $H\dot{O}_2$ radicals when compared to alkanes,[26] while at high temperatures (2000 K) it is due to the entropy loss associated with the formation of the in-plane transition state.

For an α 2° hydrogen atom in EMK, nPMK and iBMK (Fig. 9(b)) and an α 3° hydrogen atom

in iPMK (Fig. 9(c)), abstraction reactions by an $H\dot{O}_2$ radical behave similarly to the α' hydrogen atoms abstraction reactions. Abstraction of an α 2° hydrogen atom is slower than an alkane[26] by an average factor of 13 at 500 and 2000 K. For an α 3° hydrogen atom, abstraction is slower in ketones by a factor of 14 and 13 at 500 K and 2000 K, respectively, when compared to alkanes.[26]

A similar behavior is observed for the abstraction by an $H\dot{O}_2$ radical of a β 1° hydrogen atom in EMK and iPMK (Fig. 9(d)) and a β 2° hydrogen atom in nPMK (Fig. 9(e)). β 1° hydrogen atom abstraction is slower than an alkane[26] throughout the whole temperature range by a factor of 4 and 7 at 500 K and 2000 K, respectively. For a β 2° hydrogen atom, abstraction is a factor of 6 and 10 slower at 500 K and 2000 K, respectively, when compared to alkanes.[26] In iBMK, calculated rate constants for β 3° hydrogen atom abstraction by an $H\dot{O}_2$ radical (Fig. 9(f)) are slower than alkanes[26] by a factor of 4 at 500 K and 11 at 2000 K. The formation of the in-plane transition state at the γ, γ' positions of iBMK contributes to the rate constants being a factor of 2 slower than abstraction from the γ position of nPMK throughout the whole temperature range. When comparing to alkanes[26] it is observed that abstraction from the γ position of nPMK and γ, γ' positions of iBMK is slower by an average factor of 2 and 5 at 500 K and 2000 K, respectively (Fig. 10(a)).

We have calculated the average high-pressure limit rate constants for the different types of hydrogen atoms (primary, secondary or tertiary) at the different positions relative to the carbonyl group of the ketone (α', α, β and γ) and they are detailed in Table 3. Table 4 shows the Arrhenius parameters for the total rate constants for DMK, EMK, nPMK, iPMK and iBMK.

Fig. 10(b) shows the calculated average reactivity of the different types of hydrogen atoms (1°, 2° and 3°). It is not surprising that 3° hydrogen atoms are the most reactive and the 1° hydrogen atoms the least.

When comparing the calculated rate constants of hydrogen atom abstraction by an $H\dot{O}_2$ radical of ketones at the α', α, β, β' and γ, γ' positions with the rate constants calculated by Carstensen *et al.*,[27] for alkanes, it can be observed that the reactions of ketones with the $H\dot{O}_2$ radical are much slower throughout the whole temperature range. This is mostly due to the lower energy barrier for

the hydrogen atom abstraction in alkanes + $H\dot{O}_2$ radical calculated by Carstensen *et al.* than in ketones + $H\dot{O}_2$ radical. See Table 5 for detailed comparison of the relative energies.

Table 5: Comparison of the average energy barriers of the reactions of ketones + $H\dot{O}_2$ radical with the relative energies of the reactions of alkanes + $H\dot{O}_2$ radical, used in the rate constant calculations, in kcal mol^{-1}.

$H\dot{O}_2$ abstraction	Primary hydrogen atom	Secondary hydrogen atom	Tertiary hydrogen atom
This work	28.7	25.2	21.3
Aguilera-Iparraguirre *et al.*	19.5	15.4	13.7
Carstensen *et al.*	14.4	10.7	8.4

Table 6: Geometries and relative energies obtained at CCSD(T)/cc-pVTZ//MP2/6-311G(d,p) level of α' hydrogen atom abstraction transition states.

Transition state	r(C–H)/Å	r(H–O)/Å	∠(C-H-O)/Å	E/kcal mol^{-1}
TS1a	1.327	1.151	167.303	20.2
TS1b	1.324	1.155	167.257	19.7
TS1c	1.323	1.156	167.247	19.6
TS1d	1.325	1.155	166.750	19.1
TS1e	1.323	1.155	167.330	19.6
TS2a	1.329	1.148	158.353	20.4
TS2b	1.326	1.152	158.313	19.9
TS2c	1.325	1.152	158.224	19.9
TS2d	1.326	1.153	157.914	19.4
TS2e	1.324	1.153	158.414	19.9

We estimate that the overall uncertainty in the calculated rate constants is a factor of three. This is due to uncertainties in the electronic energy calculations, tunneling effects, treatment of some critical internal rotation modes, *etc*.

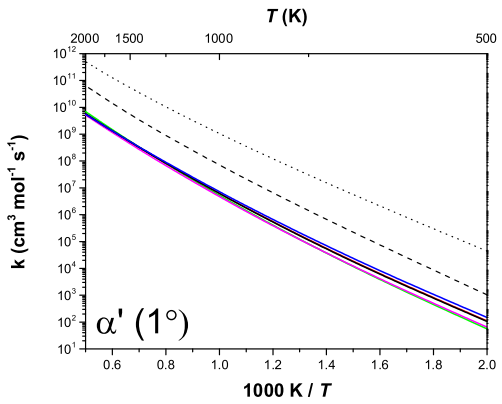

(a) Rate constants for α' 1° H atom: — DMK + $H\dot{O}_2$; — EMK + $H\dot{O}_2$; — nPMK + $H\dot{O}_2$; — iPMK + $H\dot{O}_2$; — iBMK + $H\dot{O}_2$; alkanes + $H\dot{O}_2$: ···· Cartensen *et al.*; - - Aguilera-Iparraguirre *et al.*

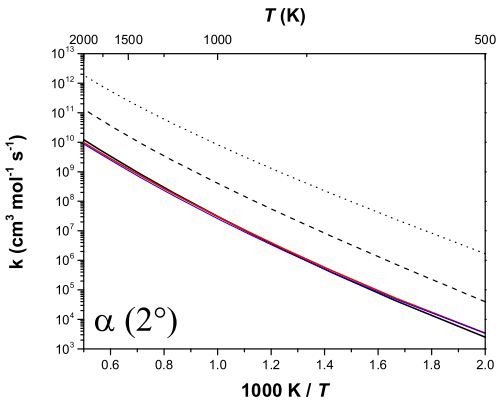

(b) Rate constants for α 2° H atom: — EMK + $H\dot{O}_2$; — nPMK + $H\dot{O}_2$; — iBMK + $H\dot{O}_2$; alkanes + $H\dot{O}_2$: ···· Cartensen *et al.*; - - Aguilera-Iparraguirre *et al.*

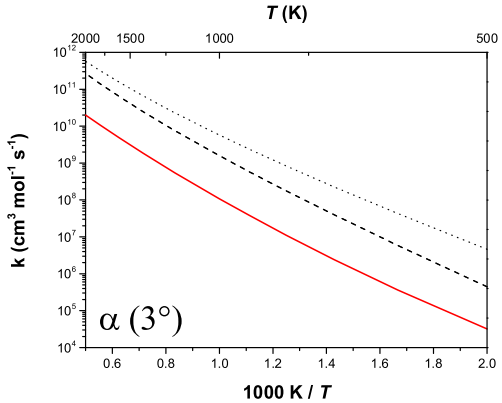

(c) Rate constants for α 3° H atom: — iPMK + $H\dot{O}_2$; alkanes + $H\dot{O}_2$: ···· Cartensen *et al.*; - - Aguilera-Iparraguirre *et al.*

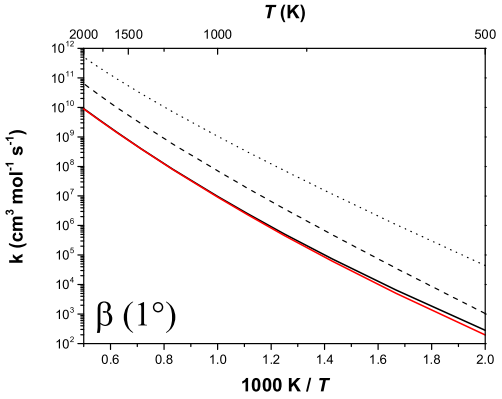

(d) Rate constants for β 1° H atom: — EMK + $H\dot{O}_2$; — iPMK + $H\dot{O}_2$; alkanes + $H\dot{O}_2$: ···· Cartensen *et al.*; - - Aguilera-Iparraguirre *et al.*

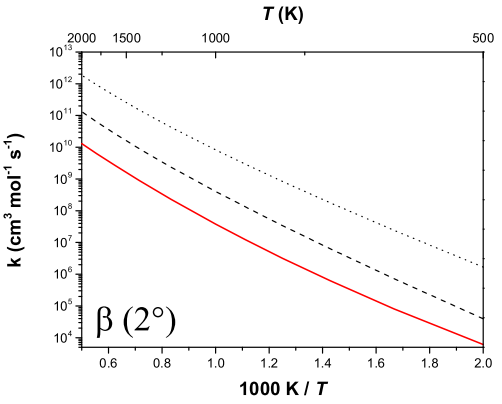

(e) Rate constants for β 2° H atom: — nPMK + $H\dot{O}_2$; alkanes + $H\dot{O}_2$: ···· Cartensen *et al.*; - - Aguilera-Iparraguirre *et al.*

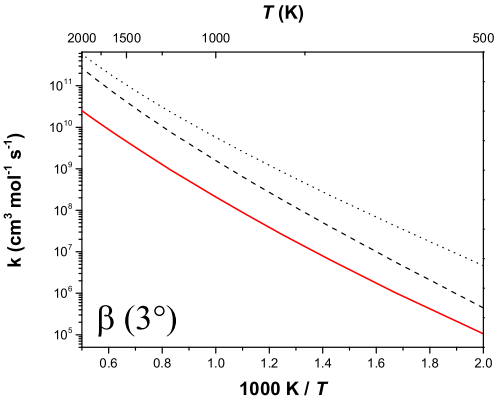

(f) Rate constants for β 3° H atom: — iBMK + $H\dot{O}_2$; alkanes + $H\dot{O}_2$: ···· Cartensen *et al.*; - - Aguilera-Iparraguirre *et al.*

Figure 9: Rate constants at the α', α and β positions for the reactions of ketones with the $H\dot{O}_2$ radical, in kcal mol^{-1}.

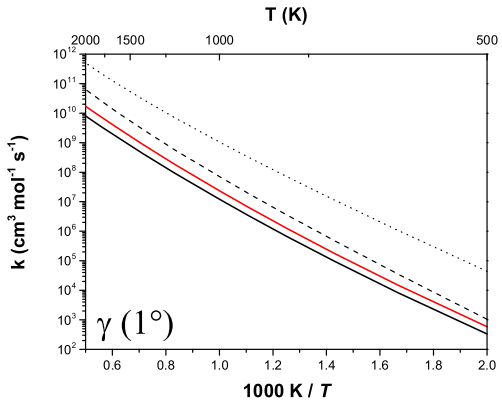

(a) Rate constants for γ 1° H atom: — nPMK + $H\dot{O}_2$; — iBMK + $H\dot{O}_2$; alkanes + $H\dot{O}_2$: ···· Cartensen *et al.*; - - Aguilera-Iparraguirre *et al.*

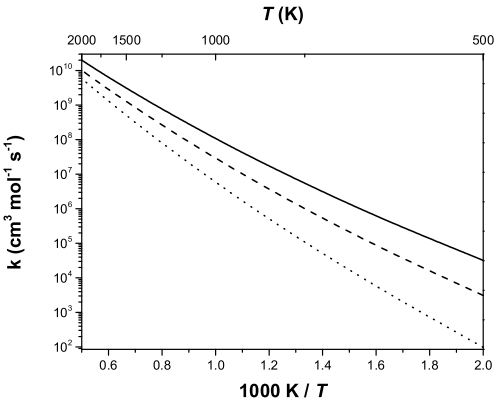

(b) A comparison of the average rate constants for abstraction of a ···· 1°, - - 2° and — 3° hydrogen atom.

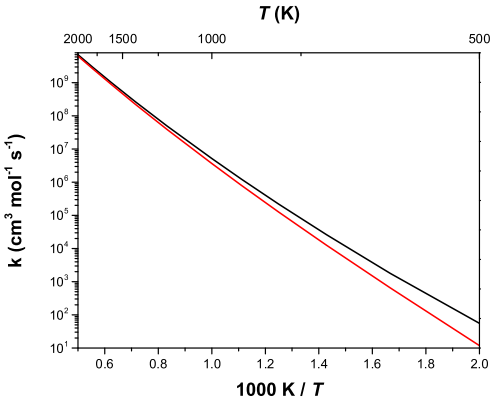

(c) A comparison of the rate constants with (—) and without (—) tunneling correction for abstraction of an α' 1° hydrogen atom for the reactions of DMK with the $H\dot{O}_2$ radical.

Figure 10: Rate constants at the γ position for the reactions of ketones with the $H\dot{O}_2$ radical, a comparison of the average rate constants for abstraction of a 1°, 2° and 3° hydrogen atom, in kcal mol^{-1} and a comparison of the rate constants with and without tunneling correction for abstraction of an α' 1° hydrogen atom for the reactions of DMK with the $H\dot{O}_2$ radical.

Conclusions

A systematic detailed study of the potential energy diagrams and reaction mechanisms of hydrogen atom abstraction by an $H\dot{O}_2$ radical on DMK, EMK, nPMK, iPMK and iBMK has been carried out. A stepwise mechanism which involves a reactant complex formed in the entrance channel and a product complex in the exit channel has been identified. A hydrogen bond is formed between the hydrogen atom in the hydroperoxyl ($H\dot{O}_2$) radical and the oxygen atom in the carbonyl group for the in-plane transition states and also for most reactant and product complexes. For the in-plane transition states, this hydrogen bond allows for a short-lived cyclic structure to be formed. Abstraction of a hydrogen atom subsequently occurs in both in- and out-of-plane transition states, leading to the formation of the product complexes followed by the products. Moreover, high-pressure limit rate constants have been calculated by conventional transition state theory; the comparison with the reactions of alkanes + $H\dot{O}_2$ radical studied by Aguilera-Iparraguirre *et al.* and Carstensen *et al.* has also been carried out. The in-plane transition state ties up rotors, effectively lowering the frequency factor, which subsequently lowers the calculated rate constants of the reactions of ketones with the $H\dot{O}_2$ radical at high temperatures.

When comparing the average reactivity of the different types of hydrogen atoms, it is observed that abstraction of a tertiary hydrogen atom is faster than abstraction of a secondary hydrogen atom which, in turn, is faster than abstraction of a primary hydrogen atom. At 500 K, abstraction of a secondary hydrogen atom is 32 times faster than a primary hydrogen atom, falling to 2 times faster at 2000 K. At 500 K, tertiary hydrogen atom abstraction ranges from 330 times faster than a primary hydrogen atom and 10 times faster than a secondary hydrogen atom, falling to 3 and 2 times faster at 2000 K, respectively.

Acknowledgement

This work was supported by Science Foundation Ireland under grant number [08/IN1./I2055]. Computational resources were provided by the Irish Center for High-End Computing (ICHEC).

Supporting Information Available

Table S1 details the CCSD(T)/cc-pV*X*Z//MP2/6-311G(d,p) (*X* = D, T, Q) single point energy calculations and extrapolation to the complete basis set limit, CCSD(T)/CBS//MP2/6-311G(d,p), for the reactions of DMK with an $H\dot{O}_2$ radical. Table S2 details optimized geometry co-ordinates and frequencies of the species involved in the rate constant calculations computed at the MP2/6-311G(d,p) level.

This material is available free of charge via the Internet at `http://pubs.acs.org/`.

References

(1) Zhou, C.-W.; Simmie, J. M.; Curran, H. J. Ab initio and Kinetic Study of the Reaction of Ketones with OH for T=500-2000 K. Part I: Hydrogen-Abstraction from $H_3CC(O)CH_{3-x}(CH_3)_x$, x = 0 → 2. *Phys. Chem. Chem. Phys.* **2011**, *13*, 11175–11192.

(2) Cours, T.; Canneaux, S.; Bohr, F. Features of the Potential Energy Surface for the Reaction of $H\dot{O}_2$ Radical with Acetone. *Int. J. Quantum Chem.* **2007**, *107*, 1344–1354.

(3) Hermans, I.; Nguyen, T. L.; Jacobs, P. A.; Peeters, J. Tropopause Chemistry Revisited: $H\dot{O}_2$*-initiated Oxidation as an Efficient Acetone Sink. *J. Amer. Chem. Soc.* **2004**, *126*, 9908–9909.

(4) Hermans, I.; Muller, J. F.; Nguyen, T. L.; Jacobs, P. A.; Peeters, J. Kinetics of Alpha-hydroxy-alkylperoxyl Radicals in Oxidation Processes. $H\dot{O}_2$-initiated Oxidation of Ketones/Aldehydes near the Tropopause. *J. Phys. Chem. A* **2005**, *109*, 4303–4311.

(5) Aloisio, S.; Francisco, J. Complexes of Hydroxyl and Hydroperoxyl Radical with Formaldehyde, Acetaldehyde, and Acetone. *J. Phys. Chem. A* **2000**, *104*, 3211–3224.

(6) Grieman, F. J.; Noell, A. C.; Davis-Van Atta, C.; Okumura, M.; Sander, S. P. Determination of Equilibrium Constants for the Reaction between Acetone and $H\dot{O}_2$ Using Infrared Kinetic Spectroscopy. *J. Phys. Chem. A* **2011**, *115*, 10527–10538.

(7) Gierczak, T.; Ravishankara, A. R. Does the $H\dot{O}_2$ Radical React with Ketones? *Int. J. Chem. Kinet.* **2000**, *32*, 573–580.

(8) Dillon, T. J.; Pozzer, A.; Vereecken, L.; Crowley, J. N.; Lelieveld, J. Does Acetone React with $H\dot{O}_2$ in the Upper-Troposphere? *Atm. Chem. Phys.* **2012**, *12*, 1339–1351.

(9) Zhou, C.-W.; Mendes, J.; Curran, H. J. Theoretical and Kinetic Study of the Reaction of Ethyl Methyl Ketone with $H\dot{O}_2$ for T = 600 - 1, 600 K. Part II: Addition Reaction Channels. *J. Phys. Chem. A* **2013**, DOI: 10.1021/jp3128127.

(10) Møller, C.; Plesset, M. S. Note on an Approximation Treatment for Many-Electron Systems. *Phys. Rev.* **1934**, *46*, 618–622.

(11) Gruneis, A.; Marsman, M.; Kresse, G. Second-order Møller–Plesset Perturbation Theory Applied to Extended Systems. II. Structural and Energetic Properties. *J. Chem. Phys.* **2010**, *133*, 074107.

(12) Gonzalez, C.; Schlegel, H. B. An Improved Algorithm for Reaction-Path Following. *J. Chem. Phys.* **1989**, *90*, 2154–2161.

(13) Pople, J. A.; Head-Gordon, M.; Raghavachari, K. Quadratic Configuration-Interaction - A General Technique for Determining Electron Correlation Energies. *J. Chem. Phys.* **1987**, *87*, 5968–5975.

(14) Peterson, K. A.; Woon, D. E.; Dunning, T. H. Benchmark Calculations with Correlated Molecular Wave-Functions .4. The Classical Barrier Height of the $H+H_2 \rightarrow H_2+H$ Reaction. *J. Chem. Phys.* **1994**, *100*, 7410–7415.

(15) Lee, T. J.; Rendell, A. P.; Taylor, P. R. Comparison of the Quadratic Configuration Interaction and Coupled-Cluster Approaches to Electron Correlation Including the Effect of Triple Excitations. *J. Phys. Chem.* **1990**, *94*, 5463–5468.

(16) J. A. Montgomery, J.; Frisch, M. J.; Ochterski, J. W.; Petersson, G. A. A Complete Basis Set Model Chemistry. VII. Use of the Minimum Population Localization Method. *J. Chem. Phys.* **2000**, *112*, 6532–6542.

(17) Merrick, J. P.; Moran, D.; Radom, L. An Evaluation of Harmonic Vibrational Frequency Scale Factors. *J. Phys. Chem. A* **2007**, *111*, 11683–11700.

(18) Frisch, M. J. et al. Gaussian 09 Revision A.1. Gaussian Inc. Wallingford CT 2009.

(19) Chemcraft v1.6 http://www.chemcraftprog.com/.

(20) Eckart, C. *Phys. Rev.* **1930**, *35*, 1303–1309.

(21) Klippenstein, S. J.; Wagner, A. F.; Dunbar, R. C.; Wardlaw, D. M.; Robertson, S. H. VariFlex, version 2.02m. Argonne National Laboratory, Argonne, IL, 1999.

(22) Pitzer, K. S.; Gwinn, W. D. Energy Levels and Thermodynamic Functions for Molecules with Internal Rotation I. Rigid Frame with Attached Tops. *J. Chem. Phys.* **1942**, *10*, 428–440.

(23) Alecu, I. M.; Zheng, J.; Papajak, E.; Yu, T.; Truhlar, D. G. Biofuel Combustion. Energetics and Kinetics of Hydrogen Abstraction from Carbon-1 in n-Butanol by the Hydroperoxyl Radical Calculated by Coupled Cluster and Density Functional Theories and Multistructural Variational Transition-State Theory with Multidimensional Tunneling. *J. Phys. Chem. A* **2012**, *116*, 12206–12213.

(24) Seal, P.; Papajak, E.; Truhlar, D. G. Kinetics of the Hydrogen Abstraction from Carbon-3 of 1-Butanol by Hydroperoxyl Radical: Multi-Structural Variational Transition-State Calculations of a Reaction with 262 Conformations of the Transition State. *J. Phys. Chem. Lett.* **2012**, *3*, 264–271.

(25) Zhou, C.-W.; Simmie, J. M.; Curran, H. J. Rate constants for hydrogen abstraction by H_2 from n-butanol. *Int. J. Chem. Kinet.* **2012**, *44*, 155–164.

(26) Aguilera-Iparraguirre, J.; Curran, H. J.; Klopper, W.; Simmie, J. M. Accurate Benchmark Calculation of the Reaction Barrier Height for Hydrogen Abstraction by the Hydroperoxyl Radical from Methane. Implications for C(n)H(2n+2) where n = 2 $\rightarrow$ 4. *J. Phys. Chem. A* **2008**, *112*, 7047–7054.

(27) Carstensen, H. H.; Dean, A. M.; Deutschmann, O. Rate Constants for the H Abstraction from Alkanes (R-H) by $R\dot{O}_2$ radicals: A Systematic Study on the Impact of R and R'. *Proc. Combust. Inst.* **2007**, *31*, 149–157.